NJC

Accepted Manuscript

This is an *Accepted Manuscript*, which has been through the Royal Society of Chemistry peer review process and has been accepted for publication.

Accepted Manuscripts are published online shortly after acceptance, before technical editing, formatting and proof reading. Using this free service, authors can make their results available to the community, in citable form, before we publish the edited article. We will replace this *Accepted Manuscript* with the edited and formatted *Advance Article* as soon as it is available.

You can find more information about *Accepted Manuscripts* in the Information for Authors.

Please note that technical editing may introduce minor changes to the text and/or graphics, which may alter content. The journal's standard Terms & Conditions and the Ethical guidelines still apply. In no event shall the Royal Society of Chemistry be held responsible for any errors or omissions in this *Accepted Manuscript* or any consequences arising from the use of any information it contains.

ROYAL SOCIETY OF CHEMISTRY

www.rsc.org/njc

NJC

PAPER

Achieving accelerated osteogenic differentiation via novel magnesium silicate hollow spheres

Received 17th August 2015,
Accepted 30th September 2015

DOI: 10.1039/x0xx00000x

www.rsc.org/njc

Baixiang Wang, Yu Wang, Chuanxia Liu, Xiaoxia Feng, Guoli Yang, and Huiming Wang*

Nanomaterials have been widely used as multifunctional scaffolds and carriers in bone tissue engineering resulting from their versatile functionalities. Here, a classical Stöber method that combined the merits of organic reagent-free hydrothermal route was introduced to rationally design and synthesize novel magnesium silicate hollow spheres (denoted as $MgSiO_3$ hollow spheres). Due to the presence of mineral elements including silicon and magnesium, these well-prepared hollow structures exhibited positive effects in accelerated osteogenic differentiation. By using an osteoblastic cell line as example, namely MC3T3-E1, we investigated the in vitro toxicity of these hollow spheres via various classical methods including MTT assay, LDH assay, apoptosis, and morphology observation. Results indicated that these materials revealed extremely low systemic toxicity and high bio-compatibility. Moreover, cellular internalization observation demonstrated that these hollow spheres could be uptaken by MC3T3-E1 cells in a time-dependent manner. This vigorous process of endocytosis could provide more raw materials for the following intracellular mineralization and bone regeneration. Results of ALP analysis and alizarin red staining indicated that these hollow spheres could clearly promote osteoblast differentiation and mineralization in a dose-dependent manner. Our study suggested that these magnesium silicate hollow spheres could act as promising candidates for enhanced bone regeneration and bone tissue engineering.

Introduction

Over the past two decades, nanomaterials have become one of the hottest topic researches around the world. Due to their tunable physico-chemical properties, admirable architectures, and simple functionalization, newly developed nanostructures have emerged as powerful candidates in a wide range of usages including drug delivery, molecular imaging, waste removal, as well as efficient catalysis.[1-10] Among all these mentioned applications, several well-fabricated nanomaterials such as graphene oxide, synthetic silicate nanoplatelet, and hydroxyapatite have achieved great success in the fields of biomedicine and bioengineering.[11-15] In particular, considering their excellent biocompatibility and negligible systemic toxicity, silicon-based and magnesium-based materials have exhibited more potential in the fields of bone reconstruction.[16-18]

The trace mineral silicon is the second most abundant element on earth and is present in all body tissues, particularly high in bone and connective tissue.[19,20] Magnesium is the fourth most abundant element in human body and more than a half of magnesium located in the bone tissue.[21] It is well known that silicon supplementation can improve bone mineral density and bone metabolism in ovariectomized rats.[22,23] Meanwhile, magnesium plays an important role in the development of bone tissue via promoting the adhesion and growth of osteoblasts.[24] Thus, both silicon and magnesium possess positive biological activity in the process of bone formation and construction. Based on above statements, it is a crucial pursuit to develop novel biomaterials containing silicon and magnesium elements for bone repair and substitution. Remarkablely, several rencent studies have demonstrated that mesoporous magnesium silicate scaffolds could benefit the adhesion and growth of osteoblast, as well as promote the differentiation of osteoblasts.[25,26] Furthermore, composite scaffolds formed with magnesium silicate and PCL–PEG–PCL molecules could be implanted into bone defects of rabbits to enhance the efficiency of new bone formation.[27] These excited results promised that biomaterials based on magnesium silicate could act as excellent candidates for bone regeneration. Although promising, these approaches are usually limited by difficulties in sample preparation, complicated synthesis routes, as well as rigorous experiment conditions such as high press or high temperature. More importantly, these bulk materials could not be directly and easily uptaken by osteoblasts, which thus prolonged the period of bone repair and seriously restricted their potential usages both in vitro and in vivo. Taking together, the development of efficient biomaterials with smaller size via a facile route for osteogenic differentiation and bone regeneration is still in high demand.

Currently, a series of magnesium silicate spheres have been rationally designed and synthesized by serveral groups including us, which could be applied as nanoscale drug carriers,

Affiliated Hospital of Stomatology, Medical College, Zhejiang University, Hangzhou 310000, P. R. China.
Email: whmzju@126.com; Fax: +86-571-87217008.
Baixiang Wang and Yu Wang contributed equally.
Electronic Supplementary Information (ESI) available: supporting figures. See DOI: 10.1039/x0xx00000x

adsorption materials, and catalyzer supporting medium in several research fields.[28-32] Remarkablely, these materials possessed the same mineral elements as those of previously reported magnesium silicate-based bioceramics and composite scaffolds. Accordingly, we envision that these spheres could be promising candidates for promoting osteogenesis by taking advantage of their unique features.

Herein, by utilizing nanoscale magnesium silicate hollow spheres as a new generation of biomaterials for intracellular mineralization, we report a simple yet efficient strategy for accelerated osteogenic differentiation in vitro. As illutrated in Fig. 1, these hollow spheres were prepared via a two-step method without any organic reagents. Then, we investigated the in vitro toxicity detailedly and traced the long-term process of intracellular mineralization. As expected, these nanoscale materials could be uptaken by osteoblasts and overcome the limitations of traditional bioceramics with unsuitable bulk. In addition, results of ALP analysis and alizarin red staining indicated that these hollow structures could clearly promote the differentiation of MC3T3-E1 cells in a dose-dependent manner. To the best of our knowledge, the present study was the first example that nanoscale magnesium silicate could efficiently enhance the intracellular mineralization. Thus, we foresee that this novel concept by using nanoscale magnesium silicate as promising candidates for osteogenic differentiation may hold great potential for biomedical usage, especially for bone regeneration and medical implantation.

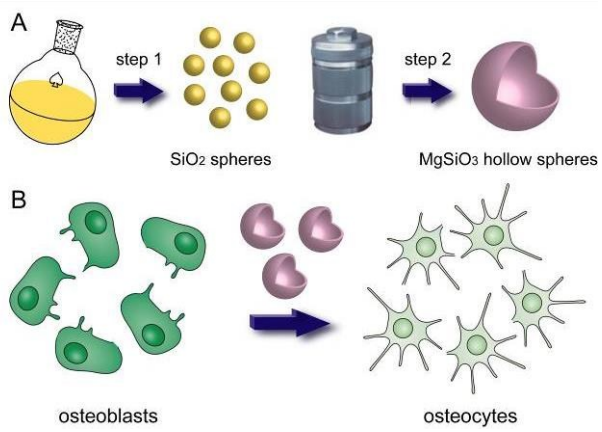

Fig. 1 Schematic illustration of the two-step synthesis of magnesium silicate hollow spheres (A) and their potential usage in accelerated osteogenic differentiation (B).

Experimental details

Chemicals

Magnesium chloride hexahydrate ($MgCl_2·6H_2O$), ammonia chloride (NH_4Cl), ammonium hydroxide aqueous solution (28%), ethanol, and tetraethyl orthosilicate were purchased from Beijing Chemical Reagents Company (Beijing, China).

Synthesis of magnesium silicate hollow spheres

Magnesium silicate hollow spheres were synthesized via a two-step route. Firstly, monodispersed silica colloidal spheres with an average diameter of 380 nm were prepared according to the classic Stöber method.[33] Then, silica colloidal spheres (100 mg) were dispersed homogeneously in deionized water (20 mL). NH_4Cl (10 mmol), $MgCl_2·6H_2O$ (0.75 mmol), and ammonia solution (1 mL) were dissolved in deionized water (20 mL). Above solution was mixed and transferred into a Teflon-lined stainless-steel autoclave (50 mL) and sealed to heat at 160 °C. After reaction for 12 h, stainless-steel autoclave was cooled to room temperature naturally. Magnesium silicate hollow spheres were rinsed with deionized water and ethanol in sequence, and dried in vacuum at 60 °C overnight. Time-dependent formation of $MgSiO_3$ were obtained via stopping the reaction at expected time points.

Synthesis of FITC-modified $MgSiO_3$ hollow spheres

FITC-modified $MgSiO_3$ hollow spheres were synthesized in accordance with our previous study.[28]

Cell culture

MC3T3-E1 pre-osteoblasts of mice were obtained from the Chinese Academy of Sciences Cell Bank (Shanghai, China). Cells were cultured in a-MEM (Gibco, USA) containing 10% fetal bovine serum (FBS), penicillin (100 U/mL) and streptomycin (100 mg/mL) in a humidified incubator of 5% CO_2 at 37°C.

Cytotoxicity analysis

MTT assays were performed to quantify the cytotoxicity of $MgSiO_3$ hollow spheres. In a typical procedure, MC3T3-E1 cells were cultured in 96-well plates as a density of 5×10^3 per well for 12 h to allow the attachment of cells. Subsequently, different concentration of $MgSiO_3$ were added into the culture medium. 1 d or 2 d after incubation with hollow spheres, MTT reagent was added into each well and incubated for another 4 h. Supernatant was removed and the formazan crystals were dissolved by the addition of DMSO. The absorbance at 490 nm was measured via a microplate reader (SpectraMax M5 Microplate Reader, Molecular Devices, USA).

Lactate dehydrogenase (LDH) release assay

MC3T3-E1 cells were incubated with different concentration of $MgSiO_3$ hollow spheres. 1 d or 2 d after incubation, culture media (50 μL) of above samples were taken out to detect LDH activity via LDH kit (Jiancheng, China). The absorbance at 450 nm was measured by a microplate reader.

Dual staining

MC3T3-E1 cells with were plated in a 12-well plate for 6 h to allow the attachment. After cells were washed twice via NaCl solution (0.9%), $MgSiO_3$ hollow spheres with different concentrations were added into above culture medium. 24 h or 48 h after incubation, cells were stained with calcein AM and propidium iodide to confirm the visualized cellular viability.

Fluorescence images were collected on an Olympus BX-51 optical system (Tokyo, Japan).

Apoptosis assays

MC3T3-E1 cells were incubated with $MgSiO_3$ hollow spheres for 2 d, washed twice with NaCl solution (0.9%), and harvested by trypsinization. After careful centrifugation, cell pellets were washed and re-suspended in binding buffer. Annexin V-FITC (5 μl) and propidium iodide (5 μl) were added. After incubating for 15 min at room temperature in dark, cells were analyzed by flow cytometer (FC500MCL, Beckman Coulter, USA).

Cytoskeletal and nuclear morphology

MC3T3-E1 cells were cultured in a 6-well plate for 12 h to allow the attachment. $MgSiO_3$ hollow spheres with different concentrations were added into above culture medium. 2 d after incubation, cells were fixed in paraformaldehyde (4%) for 15 min. After three washes with cool NaCl solution (0.9%), cells were incubated with FITC-Phalloidin (Sigma, USA) for 1 h and counterstained with Hoechst 33258 (Beyotime, China) for 10 min. Cell morphology and spreading was observed via an Olympus BX-51 optical system.

Time-dependent cellular internalization

FITC-modified $MgSiO_3$ hollow spheres were applied to carried out endocytosis study. MC3T3-E1 cells were plated in a 12-well plate for 6 h to allow the attachment. FITC-modified hollow spheres (100 μg/mL) were added into above culture medium. At expected time points, cells were washed with NaCl solution (0.9%), stained with LysoTracker Red, and observed under an Olympus BX-51 optical system. Moreover, fluorescence of FITC in the cells was detected via flow cytometer.

Alkaline phosphatase (ALP) activity

MC3T3-E1 cells with a density of 2×10^4 per well were cultured in 6-well plates. Osteogenic medium was modified with the addition of β-glycerophosphate (10 mM) and ascorbic acid (0.05 mM). $MgSiO_3$ hollow spheres were added into above culture medium. 5, 10, and 15 days after incubation, NaCl solution (0.9%) containing Triton X-100 (1%) was used to dissolve out cellular proteins. After careful centrifugation, the supernatants were subjected to protein content measurement and ALP activity by using a bicinchoninic acid (BCA) protein assay kit and an ALP activity kit (Jiancheng, China). All the results were normalized by the protein content.

Alizarin red staining

MC3T3-E1 cells with a density of 1×10^5 per well were cultured in 6-well plates. $MgSiO_3$ hollow spheres were added into above culture medium. 3 weeks after incubation, cells were fixed in ethanol (95%) at 4 °C for 10 min, stained with alizarin red S (2%) for 30 min, then washed with NaCl solution (0.9%). Photos were collected on an Olympus BX-51 optical system. Quantitative analysis was carried out by elution with cetylpyridium chloride (10% w/v) for 10 min. Then, the absorbance was measured at 570 nm using a microplate reader.

Result and discussion

Formation of $MgSiO_3$ hollow spheres

Fig. 1A demonstrated that our system combined a classical Stöber method for the formation of SiO_2 colloidal spheres and a facile hydrothermal approach for the growing of $MgSiO_3$ hollow structures on the basis of a chemical-template etching mechanism. Specifically, SiO_2 colloidal spheres incubated with an alkaline solution containing magnesium ions, ammonium ions and ammonia were transferred to a Teflon-lined stainless-steel autoclave. Upon a high-temperature treatment, the silica chains were broken by hydroxide ions and then generated silicate-ion groups. The magnesium ions reacted with silicate ions released from SiO_2 colloidal spheres to construct $MgSiO_3$ in situ around the SiO_2 cores. Followed by the gradual release of silicate ions, well-structured $MgSiO_3$ hollow spheres were finally formed along with the time passing.[29,31,34-36]

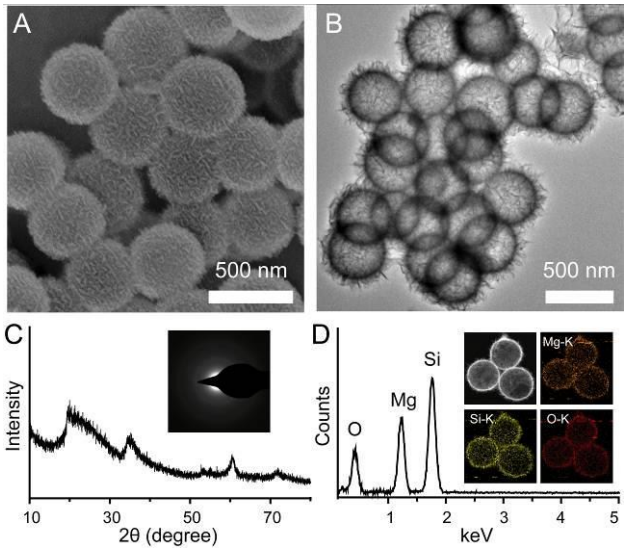

Fig. 2 SEM image (A), TEM image (B), wide-angle XRD pattern (C), and EDS spectrum (D) of $MgSiO_3$ hollow spheres. Inset of C: SAED image. Inset of D: EDS elemental distribution maps of Mg, Si, and O signals.

Morphological and structural features of $MgSiO_3$ hollow spheres were examined via scanning electron microscopy (SEM) and transmission electron microscopy (TEM). As exhibited in Fig. 2A and Fig. 2B, observation of the SEM and TEM images showed the surface of $MgSiO_3$ revealed needle-like structures at first glance, which were constituted of large, narrow, and nanoscale lamellae. The average diameter of these well-prepared hollow spheres was nearly 400 nm. Crystalline order and phase purity have been considered as two of the most significant parameters affecting the properties of materials.

Wide-angle XRD patterns and SAED image shown in Fig. 2C demonstrated that all the well-defined diffraction peaks exhibited the features of $MgSiO_3$ (JCPDS No. 03-0174).[29,31] Energy-dispersive spectroscopy (EDS) spectrum and elemental istribution maps of $MgSiO_3$ hollow spheres figured out the presence of Mg, Si, and O elements in these hollow structures (Fig. 2D). In addition, these samples held a hollow structure with an obviously darkish center and black edge based on TEM image and elemental distribution maps. N_2 adsorption and desorption analysis was then introduced to examine the pore properties of these hollow structures. As shown in Fig. S1, N_2 adsorption–desorption isotherms revealed a typical IV-type isotherm, suggesting the presence of mesopores. According to above isotherm, these hollow spheres exhibited a narrow pore size distribution with homogeneous pores about 4.32 nm and a high specific surface area of 498 m^2/g.

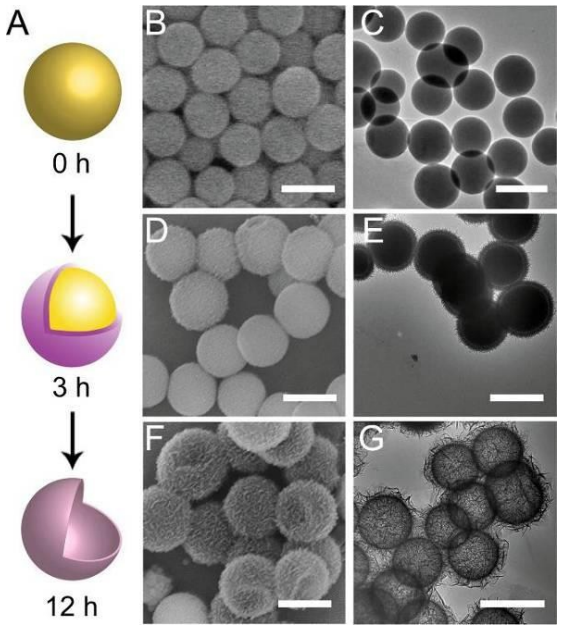

Fig. 3 Schematic illustration of the time-dependent formation of $MgSiO_3$ hollow spheres (A), as well as related SEM (B) and TEM images (C). The scale bar is 500 nm.

To benifit the understanding of readers, time-dependent experimentals were designed and peformed to investigate the formation process of these hollow spheres. As shown in Fig. 3A, SiO_2 colloidal spheres were uniform with a diameter of 380 nm and a related smooth surface without any reaction. After 3 h of the reaction, SiO_2 colloidal spheres were dissolved by OH^- due to the destruction of silicon-oxygen chains on the surface. Moreover, thin and total magnesium silicate shells around the SiO_2 cores were formed at the same time. After 12 h of the reaction, all the SiO_2 cores were completely dissolved, which resulted in the void structure at last. Complementary SEM and TEM images in Fig. 3B and Fig. 3C further confirmed our design. We then evaluated the dispersibility of these hollow spheres in various physiological solution. As shown in Fig. S2, these $MgSiO_3$ hollow spheres with a concentration of 0.5 mg/mL could well disperse in various aqueous solutions including NaCl solution (0.9%), FBS, and DMEM without serious aggregation. Dynamic light scattering (DLS) analysis demonstrated that these hollow spheres exhibited a mean diameter of 470 nm with a standard deviation of ±45 nm in NaCl solution (0.9%), which was suitable for further usages in biomedicine.

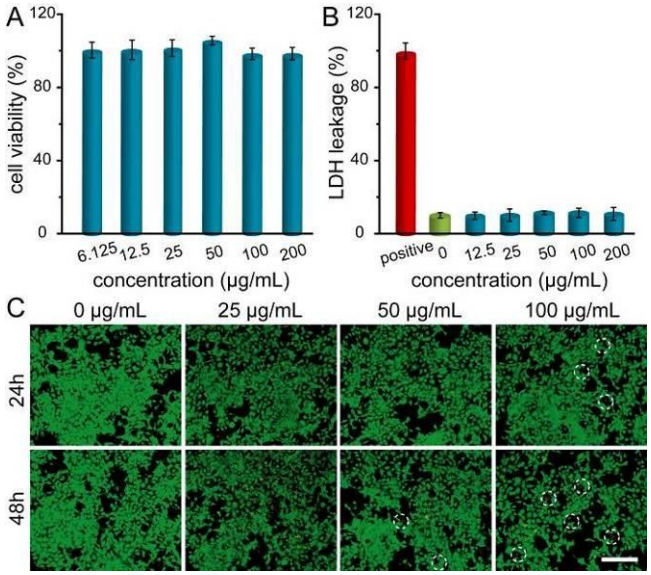

Fig. 4 Cell viability (A) and LDH leakage (B) of MC3T3-E1 cells 48 h after incubation with $MgSiO_3$ hollow spheres. Fluorescence microscopy images of calcein AM and propidium iodide co-stained cells incubated with and without $MgSiO_3$ (C). The scale bar is 200 μm.

In vitro toxicity

Prior to studying the effects on accelerated osteogenic differentiation of $MgSiO_3$ hollow spheres, MTT assay and LDH activity assay associated with osteoblastic cell line, MC3T3-E1 were investigated at first. As shown in Fig. S3A and Fig. 4A, cell viability was not hindered by these hollow structures even up to a concentration of 200 μg/mL. Otherwise, results of lactate dehydrogenase (LDH) activity induced by these hollow spheres revealed no obvious differences could be detected between negative control group (concentration: 0 μg/mL) and other experimental groups upon 24 h or 48 h of treatments (Fig. S3B and Fig. 4B). To obtain more accurate results, dual staining experiments were carried out to confirm visualized cellular viability in the presence of $MgSiO_3$ hollow spheres. As shown in Fig. 4C, nearly all the cells were still alive upon above treatments. White circles in the images indicated that slight cellular injury occured along with the increasing of $MgSiO_3$ concentrations and incubation period. Significantly, the percentages of dead cells were all less than 1%, indicating extremely high bio-compatibility of these hollow structures in vitro. Flow cytometry (FCM) was further selected to evaluate apoptosis for the additional analysis of cytotoxicity at various incubation concentrations including 25 μg/mL, 50 μg/mL and 100 μg/mL. After 48 h incubation, the data shown in Fig. 3A and Fig. S4 demonstrated that the percentage of apoptosis became larger with the increasing concentration. However,

percentages of normal cells in all these groups were still higher than 80%, which indicated that these hollow spheres could not result in serious cellular injury even upon a long-term incubation period and a high incubation concentration. More detailed nuclear and morphological changes of MC3T3-E1 cells were achieved by using fluorescence microscope method. As illutrated in Fig. 5B, microscopy images indicated that there were no obvious differences occured in the morphology of cells treated with $MgSiO_3$ hollow spheres compared to the control group. All the cellular morphology was found to be normal and exhibited a flattened appearance. White circles in the group treated with 100 μg/mL hollow spheres provided complementary evidence to describe the slight apoptosis happened. On the basis of above results, it could be summarized that there was no significant effect occured on MC3T3-E1 cells even when the incubation concentration of $MgSiO_3$ hollow spheres was increased to 100 μg/mL.

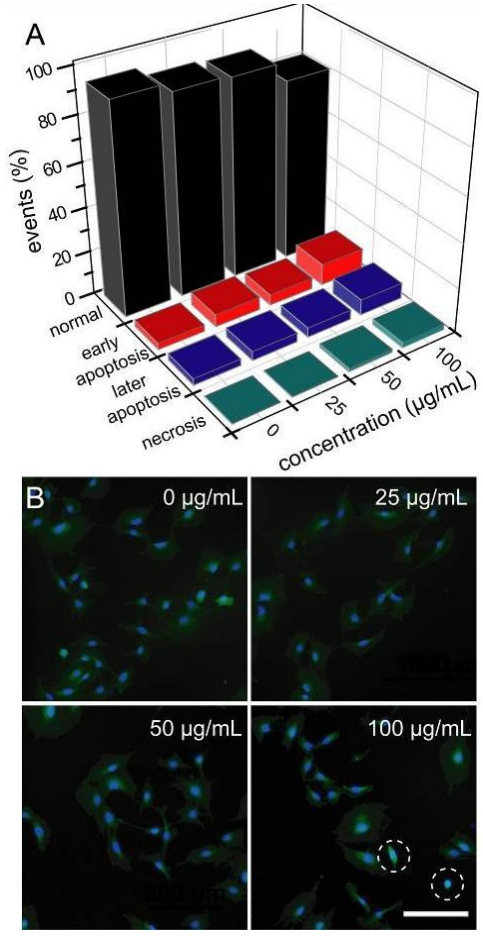

Fig. 5 Apoptosis analysis of MC3T3-E1 cells incubated with $MgSiO_3$ hollow spheres (A). Fluorescence microscopy images of cytoskeletal and nuclear morphology of cells incubated with $MgSiO_3$ (B). The scale bar is 50 μm.

Cellular uptake investigation

Concluded from previous studies, two pivotal parameters to induce cytotoxicity were the size of particles and the quantity of cellular uptake. As well known, nanoparticles with smaller size usually exhibited better cellular uptake efficiency but higher cytotoxicity than the larger ones.[16,37] Herein, we selectively and rationally designed $MgSiO_3$ hollow spheres with an average diameter of 400 nm as the final target to obtain high efficiency in cellular uptake and extremely low systemic toxicity in vitro. According to our previous study, fluorescence $MgSiO_3$ hollow spheres were firstly prepared by using FICT molecules as efficient fluorescence label. Fig. 6 illustrated the time-dependent cellular uptake of FITC-labeled $MgSiO_3$ hollow spheres. Lyso-tracker red as a famous lysosome label was applied to spatially confirm the precise position of hollow pheres. It was clearly observed that more green fluorescence of FITC could be found in the group treated with 12 h of incubation compared to other experimental groups, indicating that MC3T3-E1 cells could uptake more FITC-modified hollow spheres along with the time passing. Moreover, FCM analysis shown in Fig. S5 further recured our above results. Lysate of MC3T3-E1 cells was applied to investigated the release of Mg and Si ions from our $MgSiO_3$ hollow spheres. After incubation with different periods, we tested the concentrations of Mg and Si ions in the supernatant via ICP-MS method after careful centrifugation. It could be found that more Mg and Si ions could be released from these hollow spheres with the increasing of incubation periods (data not shown). Above ideal results could provide more opportunities for these hollow spheres in further in vitro study of osteogenic differentiation because of their high amount in cellular internalization and continuance release phenomenon of mineral ions.

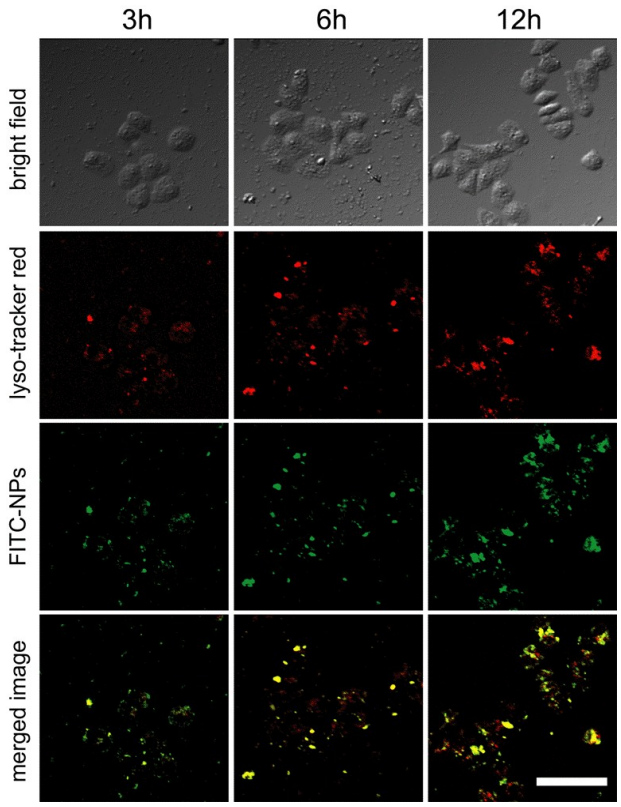

Fig. 6 Time-dependent cellular internalization of FITC-modified $MgSiO_3$ hollow spheres. The scale bar is 50 μm.

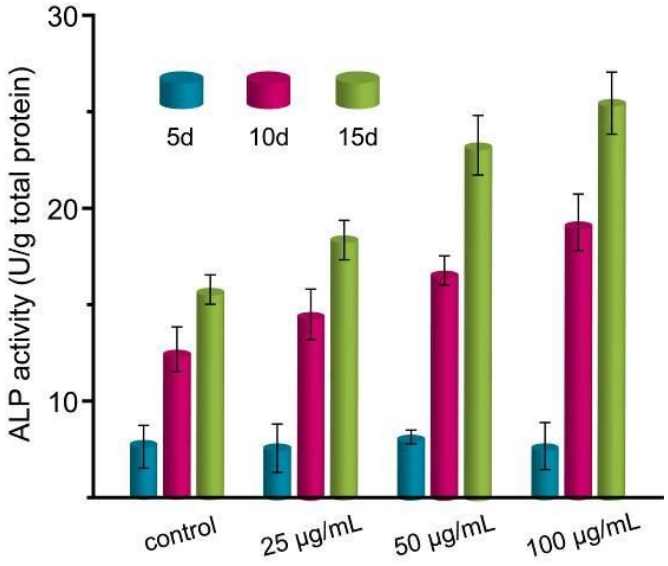

Fig. 7 ALP activity of MC3T3-E1 cells after incubation with $MgSiO_3$ hollow spheres.

Accelerated osteogenic differentiation

Admirable biomaterials for bone regeneration and bone repair must interact actively with bone cells and promote their osteogenic differentiation. Thus, we additionally investigated the influence of $MgSiO_3$ hollow spheres on the differentiation ability of MC3T3-E1 cells via detecting the expression of ALP, which could correlate with matrix formation in osteoblasts prior to the initiation of mineralization.[38-40] As exhibited in Fig. 7, ALP activity of MC3T3-E1 cells was found to increase with the incubation periods for all samples. After 5 d of incubation, no significant differences could be detected between the control group and other experimental groups. However, all groups treated with hollow spheres presented high expression f ALP activity compared with those in the control groups after 10 d and 15 d of incubation. Significantly, the highest expression of ALP activity could be found in the group with a concentration of 100 μg/mL hollow spheres after 15 d of incubation. To evaluate whether $MgSiO_3$ hollow spheres could lead to osteoblast mineralization in vitro, alizarin red staining was applied to offer primary evidence. After 21 d of incubation, MC3T3-E1 cells were stained with alizarin red S to achieve calcium deposition. As shown in Fig. 8A, positive nodules could be found in all experimental groups instead of the control group. More importantly, above process of cellular mineralization exhibited a dose-dependent manner, which could also be seriously affected by the material concentration. Thus, it was expected that by regulating the incubation period and the incubation concentration, cellular mineralization with different degrees could be obtained at the same time. Quantitative data based on three independent experiments further confirmed our results of cellular mineralization (Fig. 8B). Previous studies demonstrated that Mg and Si ions dissolved from well-fabricated biomaterials could stimulate osteoblast differentiation in vitro.[41,42] Thus, the increased ALP activity and more calcium deposition nodules after our treatment could be ascribed to the results of osteoblast differentiation in vitro. We could explained that as follows. Firstly, $MgSiO_3$ hollow spheres began to degrade after efficient intracellular uptake, which caused the release of Si and Mg ions. Second, silanol groups constructed by the released Si ions and excess H^+ in lysosome underwent polycondensation to form a silicagel layer, on which Ca^{2+} and phosphate ions adsorbed from the solution could aggregate. Finally, the reaction of these ions formed amorphous calcium phosphate layer that crystallized into apatite.[22] Taking together, these $MgSiO_3$ hollow spheres could lead to efficient differentiation and mineralization of osteoblasts in vitro, which exhibited more potential for further bone regeneration and bone repair.

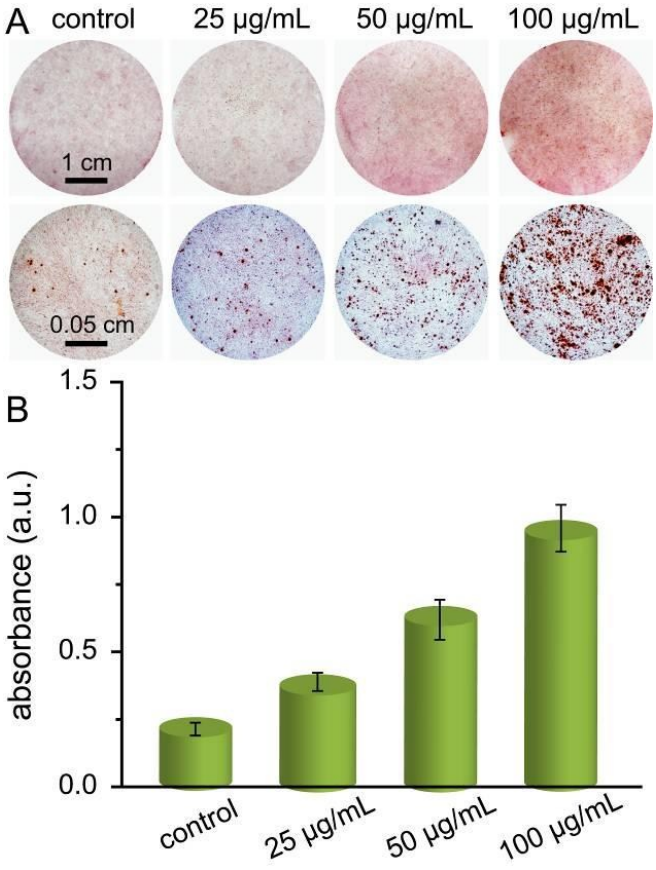

Fig. 8 Effects on mineralization of MC3T3-E1 cells via alizarin red staining 21 d after incubation with $MgSiO_3$ hollow spheres (A). Quantitative analysis of mineralization by spectrophotometery at 570 nm (B).

Conclusions

In summary, we have rationally designed novel magnesium silicate hollow spheres via a facile two-step route, and utilized them to achieve accelerated osteogenic differentiation in vitro. Detailed studies of cytotoxicity were investigated via various classical routes. Results suggested that these well-prepared hollow spheres exhibited extremely low systemic toxicity and great bio-compatibility, which thus exhibited negative effects

on the morphology and viability of MC3T3-E1 cells. Moreover, these hollow spheres could be efficiently uptaken by MC3T3-E1 cells in a time-dependent manner. ALP analysis and alizarin red staining further indicated that our materials could clearly exhibit their capability in promoting osteoblast differentiation and cellular mineralization. Last but not least, our present study provided a novel concept by using nanoscale magnesium silicate as promising candidates for osteogenic differentiation, which might hold great potential for unborn biomedical usage, especially for new bone formation and bone regeneration.

Acknowledgements

This study was financially supported by the National Natural Science Foundation of China (No. 81171003 and 81371120), China Postdoctoral Science Foundation Funded Project (NO:2015M571891) and Zhejiang Provincial Medical Science and Technology Project of China (NO:2015KYA146).

Notes and references

1 K. An and T. Hyeon, *Nano Today*, 2009, **4**, 359.
2 W. Cai and X. Chen, *Small* 2007, **3**, 1840.
3 X. Lou, Y. Wang, C. Yuan, J. Lee and L. Archer, *Adv. Mater.*, 2006, **18**, 2325.
4 R. Bardhan, S. Lal, A. Joshi and N. Halas, *Acc. Chem. Res.* 2011, **44**, 936.
5 P. Arnal, M. Comotti and F. Schüth, *Angew. Chem. Int. Ed.*, 2006, **45**, 8224.
6 Z. Liu, J. Liu, R. Wang, Y. Du, J. Ren and X. Qu, *Biomaterials,* 2015, **56**, 206.
7 G. Maltzahn, J. Park, A. Agrawal, N. Bandaru, S. Das, M. Sailor and S. Bhatia, *Cancer Res.* 2009, **69**, 3892.
8 D. Pan, C. Schirra, A. Senpan, A. Schmieder, A. Stacy, E. Roessl, A. Thran, S. Wichline, R. Proska and G. Lanza, *ACS Nano,* 2012, **6**, 3364.
9 C. Qiao, K. Zhang, H. Jin, L. Miao, C. Shi, X. Liu, A. Yuan, J. Liu, D. Li, C. Zheng, G. Zhang, X. Li, B. Yang and H. Sun, *Int. J. Nanomed.*, 2013, **8**, 2985.
10 D. Yang, Y. Dai, J. Liu, Y. Zhou, Y. Chen, C. Li, P. Ma, and J. Lin, *Biomaterials,* 2014, **35**, 2011.
11 S. Mihaila, A. Gaharwar, R. Reis, A. Khademhosseini, A. Marques and M. Gomes, *Biomaterials*, 2014, **35**, 9087.
12 M. Li, X. Yang, J. Ren, K. Qu and X. Qu, *Adv. Mater.* 2012, **24**, 1722.
13 J. Lu, Y. He, C. Cheng, Y. Wang, L. Qiu, D. Li and D. Zou, *Adv. Funct. Mater.* 2013, **23**, 3494.
14 L. Pan, J. Liu, Q. He, L. Wang and J. Shi, *Biomaterials*, 2013, **34**, 2719.
15 J. Lee, Y. Shin, O. Jin, S. Kang, Y. Hwang, J. Park, S. Hong and D. Han, *Nanoscale*, 2015, **7**, 11642.
16 X. Xu, K. Zhang, L. Zhao, D. Wang, W. Bu, C. Zheng and H. Sun, *RSC Adv.*, 2014, **4**, 46481.
17 G. BeckJr, S. Ha, C. Camalier, M. Yamaguchi, Y. Li, J. Lee and M. Weitzmann, *Nanomedicine*, 2012, **8**, 793.
18 H. Nie, M. Ho, C. Wang, C. Wang and Y. Fu, *Biomaterials*, 2009, **30**, 892.
19 Z. Mao, L. Wan, L. Hu, L. Ma and C. Gao, *Colloids Surf. B*, 2010, **75**, 432.
20 Y. Yoo and W. Lee, *Surf. Coat. Technol.*, 2012, **213**, 291.
21 S. Volpe, *Adv. Nutr.*, 2013, **4**, 378.
22 M. Kim, Y. Bae, M. Choi and Y. Chung, *Biol. Trace Elem. Res*. 2009, **128**, 239.
23 Y. Bae, J Kim, M. Choi, Y. Chung, M. Kim, *Biol. Trace Elem. Res.*, 2008, **124**, 157.
24 M. Sader, R. LeGeros and G. Soares, *J. Mater. Sci. Mater. Med.*, 2009, **20**, 521.
25 Z. Wu, T. Tang, H. Guo, S. Tang, Y. Niu , J. Zhang, W. Zhang, R. Ma, J. Su, C. Liu and J. Wei, *Colloids Surf. B*, 2014, **120**, 38.
26 Y. Niu, W. Dong, H. Guo, Y. Deng, L. Guo, X. An, D. He, J. Wei and M. Li, *Int. J. Nanomed.*, 2014, **9**, 2665.
27 D. He, W. Dong, S. Tang, J. Wei, Z. Liu, X. Gu, M. Li, H. Guo and Y. Niu, *J. Mater. Sci. Mater. Med.*, 2014, **25**, 1415.
28 B. Wang, W. Meng, M. Bi, Y. Ni, Q. Cai and J. Wang, *Dalton Trans.*, 2013, **42**, 8918.
29 Y. Wang, G. Wang, H. Wang, C. Liang, W. Cai and L. Zhang, *Chem. Eur. J.,* 2010, **16**, 3497.
30 C. Cui, Q. Wang, S. Hao, J. Qu, P. Huang, C. Cao, W. Song and Z. Yu, *ACS Appl. Mater. Interfaces*, 2014, **6**, 14653.
31 J. Zheng, B. Wu, Z. Jiang, Q. Kuang, X. Fang, Z. Xie, R. Huang and L. Zheng, *Chem. Asian J.*, 2010, **5**, 1439.
32 E. Eikeland, A. Blichfeld, C. Tyrsted, A. Jensen and B. Iversen, *ACS Appl. Mater. Interfaces*, 2015, **7**, 5258.
33 W. Stöber and A. Fink, *J. Colloid Interf. Sci.,* 1968*,* **26**, 62.
34 Y. Wang, G. Wang, H. Wang, W. Cai and L. Zhang, *Chem. Commun.*, 2008, **44**, 6555.
35 Z. Liu, M. Li, X. Yang, M. Yin, J. Ren and X. Qu, *Biomaterials*, 2011, **32**, 4683.
36 Q. Fang, S. Xuan, W. Jiang and X. Gong, *Adv. Funct. Mater*., 2011, **21**, 1902.
37 Z. Yue, W. Wei, Z. You, Q. Yang, H. Yue, Z. Su and G. Ma, *Adv. Funct. Mater.* 2011, **21**, 3446.
38 X. Bao, X. Wei, Y. Wang, H. Jiang, D. Yu and M. Hu, *Ann. Biomed. Eng.*, 2014, **42**, 1781.
39 T. Tian, Y. Han, B. Ma, C. Wu and J. Chang, *J. Mater. Chem. B*, 2015, **3**, 6773.
40 B. Choi, Z. Cui, S. Kim, J. Fan, B, Wu and M. Lee, *J. Mater. Chem. B*, 2015, **3**, 6448.
41 A. Salinas, J. Roman, M. Vallet-Regi, J. Oliveira, R. Correia and M. Fernandes, *Biomaterials*, 2000, **21**, 251-257.
42 J. Guan, J. Zhang, S. Guo, H. Zhu, Z. Zhu, H. Li, Y. Wang, C. Zhang and J. Chang, *Biomaterials*, 2015, **55**, 1.

Table of Contents

Achieving accelerated osteogenic differentiation via novel magnesium silicate hollow spheres

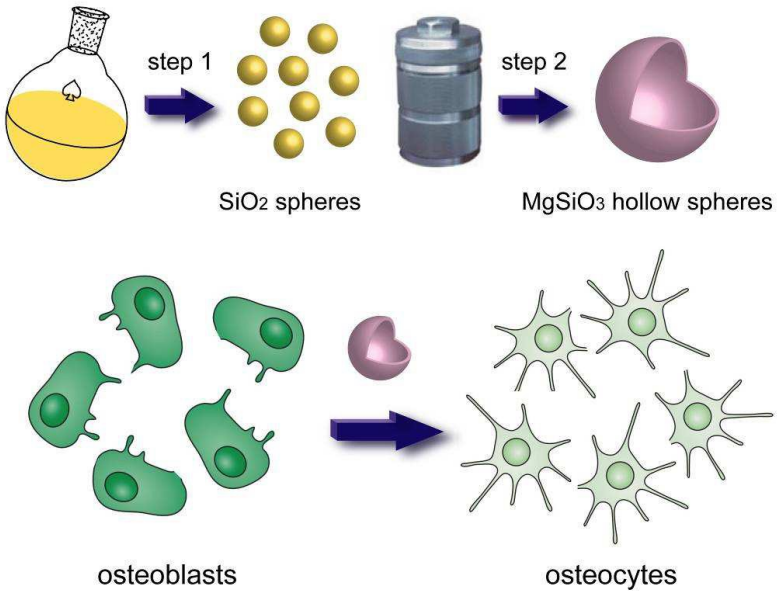

Novel $MgSiO_3$ hollow spheres have been rationally designed and applied as promising candidates for osteogenic differentiation in vitro.